01 Apr 2015

Azimuthal Anisotropy beneath North Central Africa from Shear Wave Splitting Analyses

Awad A. Lemnifi

Kelly H. Liu
Missouri University of Science and Technology, liukh@mst.edu

Stephen S. Gao
Missouri University of Science and Technology, sgao@mst.edu

Cory A. Reed

et. al. For a complete list of authors, see https://scholarsmine.mst.edu/geosci_geo_peteng_facwork/396

Recommended Citation

A. A. Lemnifi et al., "Azimuthal Anisotropy beneath North Central Africa from Shear Wave Splitting Analyses," *Geochemistry, Geophysics, Geosystems*, vol. 16, no. 4, pp. 1105-1114, John Wiley & Sons Ltd, Apr 2015.
The definitive version is available at https://doi.org/10.1002/2014GC005706

AGU PUBLICATIONS

Geochemistry, Geophysics, Geosystems

RESEARCH ARTICLE
10.1002/2014GC005706

Azimuthal anisotropy beneath north central Africa from shear wave splitting analyses

Awad A. Lemnifi[1], Kelly H. Liu[1], Stephen S. Gao[1], Cory A. Reed[1], Ahmed A. Elsheikh[1], Youqiang Yu[1], and Abdala A. Elmelade[2]

[1]Geology and Geophysics Program, Missouri University of Science and Technology, Rolla, Missouri, USA, [2]Libyan Center for Remote Sensing and Space Science, Tripoli, Libya

Key Points:
- Splitting parameters were measured for the first time in interior N. Africa
- N-S fast orientations are inconsistent with lithospheric origin
- Anisotropy is due to partial lithosphere-asthenosphere coupling

Correspondence to:
S. S. Gao,
sgao@mst.edu

Citation:
Lemnifi, A. A., K. H. Liu, S. S. Gao, C. A. Reed, A. A. Elsheikh, Y. Yu, and A. A. Elmelade (2015), Azimuthal anisotropy beneath north central Africa from shear wave splitting analyses, *Geochem. Geophys. Geosyst.*, *16*, 1105–1114, doi:10.1002/2014GC005706.

Received 29 DEC 2014
Accepted 20 MAR 2015
Accepted article online 27 MAR 2015
Published online 18 APR 2015

Abstract This study represents the first multistation investigation of azimuthal anisotropy beneath the interior of north central Africa, including Libya and adjacent regions, using shear wave splitting (SWS) analysis. Data used in the study include recently available broadband seismic data obtained from 15 stations managed by the Libyan Center for Remote Sensing and Space Science, and those from five other stations at which data are publicly accessible. A total of 583 pairs of high-quality SWS measurements utilizing the PKS, SKKS, and SKS phases demonstrate primarily N-S fast orientations with an average splitting delay time of approximately 1.2 s. An absence of periodic azimuthal variation of the observed splitting parameters indicates the presence of simple anisotropy, and lack of correlation between surficial features and the splitting parameters suggests that the origin of the observed anisotropy is primarily asthenospheric. This conclusion is enhanced by nonperiodic azimuthal variation of the splitting parameters observed at one of the stations located near the boundary of areas with different anisotropic properties. We interpret the observed anisotropy to be the consequence of northward movement of the African plate relative to the asthenosphere toward the Hellenic and Calabrian subduction zones. Local variance in fast orientations may be attributable to flow deflection by the northern edge of the African continental root. The observations provide critical and previously lacking constraints on mantle dynamic models in the vicinity of the convergent boundary between the African and Eurasian plates.

1. Introduction

Numerous geodynamic modeling and seismic anisotropy studies suggest that the rheologically different lithosphere and asthenosphere interact through partial coupling [*Becker and O'Connell*, 2001; *Marone and Romanowicz*, 2007; *Doglioni et al*., 2011; *Refayee et al*., 2014; *Yang et al*., 2014]. The direction of the simple shear in the boundary layer between the partially coupled lithosphere and asthenosphere is determined by the relative velocities between the two layers. Mathematically, the resulting shear direction at the boundary layer is determined by the vector sum of the two velocities [*Conrad and Behn*, 2010].

The interaction between the lithosphere and asthenosphere is routinely investigated using geodynamic modeling, with constraints from geophysical observations. Shear wave splitting (SWS) parameters (fast polarization orientation ϕ and splitting time δt) obtained using P-to-S converted phases at the core-mantle boundary (XKS including PKS, SKKS, and SKS) are arguably the most relevant and consequently most frequently used seismic observations [*Becker et al*., 2006; *Bird et al*., 2008; *Kreemer*, 2009; *Conrad and Behn*, 2010; *Forte et al*., 2010; *Faccenna et al*., 2014]. Laboratory, field, and numerical experiments suggest that when anisotropic minerals in the mantle (primarily olivine) are subjected to deformation, lattice preferred orientation (LPO) will be developed through dislocation creep [*Zhang and Karato*, 1995]. When a shear wave travels through an anisotropic medium, it splits into two orthogonal waves, one traveling faster than the other [e.g., *Silver*, 1996; *Savage*, 1999]. Under anhydrous conditions with typical mantle temperature, the polarization orientation most often corresponds to the prevailing direction of simple shear [*Karato et al*., 2008].

The mantle flow field associated with the subducting African plate beneath the Mediterranean Sea and adjacent areas has recently been intensively investigated through geodynamic modeling [e.g., *Faccenna and Becker*, 2010; *Schaefer et al*., 2011; *Faccenna et al*., 2014], using available SWS measurements [*Barruol and Hoffmann*, 1999; *Schmid et al*., 2004; *Miller et al*., 2013] as constraints. Most of the SWS measurements

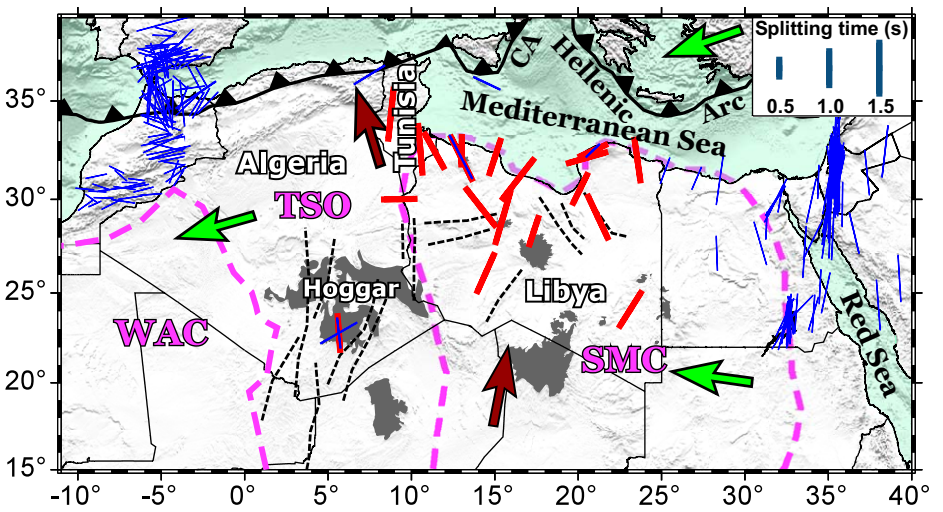

Figure 1. A digital elevation map of northern Africa showing station-averaged shear wave splitting measurements from this study (red bars), major basement faults (dashed black lines) [*Guiraud and Bosworth*, 1997], boundaries of major tectonic provinces (dashed magenta lines), and Cenozoic volcanic centers (dark gray areas). SMC: Saharan Metacraton; TSO: Trans-Saharan Orogen; WAC: West African Craton; CA: Calabrian Arc. Also shown are splitting parameters from previous shear wave splitting studies (blue bars) [*Diaz et al.*, 1998; *Barruol and Hoffmann*, 1999; *Barruol and Ismail*, 2001; *Schmid et al.*, 2004; *Hansen et al.*, 2006; *Buontempo et al.*, 2008; *Diaz et al.*, 2010; *Kaviani et al.*, 2011, 2013; *Salah*, 2012; *Miller et al.*, 2013; *Diaz and Gallart*, 2014; *Elsheikh et al.*, 2014]. The dark red arrows represent plate motion of Africa relative to Eurasia calculated using the NUVEL-1A model [*DeMets et al.*, 1994], and the green arrows show APM vectors determined by the HS3-NUVEL1A model [*Gripp and Gordon*, 2002].

are on the Eurasian and Arabian plates. The limited number of measurements on the African plate are restricted mostly to the coastal area of the Mediterranean Sea, and measurements in the interior of north central Africa are rare. Here we use newly obtained data from 15 seismic stations located throughout the interior and northern coast of Libya as well as five public seismic stations in Libya and surrounding areas (Figure 1) to constrain the origin of anisotropy and thus characterize the nature of deformation and mantle flow beneath north central Africa.

1.1. Tectonic Setting

The African plate is largely composed of a number of terranes, among which the largest ones are the West African Craton (WAC) and the Saharan Metacraton (SMC). They were amalgamated by a span of orogenic events collectively known as the Neoproterozoic Pan-African orogeny [*Stoeser and Camp*, 1985; *Stern*, 1994] (Figure 1). As a consequence, northern Africa is underlain by lithosphere with variable thickness owing to extensive Pan-African orogenic suturing of blocks with a diverse set of tectonic environments [*Stern*, 1994]. Beneath north central Africa, these tectonic entities are permeated by a variety of major basement faults and corresponding fold belts primarily oriented N-S or NW-SE (Pan-African Orogenesis) and NE-SW (Carboniferous Hercynian compressional stresses) [*Hassan and Kendall*, 2014] (Figure 1).

The northern reaches of Africa are dominated by volcanic provinces (Figure 1), the most notable of which is the Hoggar swell of Algeria [*Liégeois et al.*, 2003] located in the region between the boundaries of the SMC and WAC known as the Trans-Saharan Orogen (TSO). Hoggar volcanics, like other Cenozoic basaltic outpourings across northern Africa, are thought to be the result of shallow asthenospheric upwelling exploiting preexisting lithospheric heterogeneities rather than deep-mantle origins [*Montagner et al.*, 2007; *Meert and Lieberman*, 2008]. Farther to the north, beyond the Mediterranean rifted margin, the Calabrian and Hellenic subduction zones comprise the northern extent of the northern African subduction system [*Faccenna et al.*, 2014] (Figure 1).

1.2. Previous Geophysical Studies Beneath North Central Africa

High-resolution investigations of crustal and mantle structure beneath north central Africa are relatively limited as a consequence of sparse broadband seismic data coverage in the area. A global tomography study [*Grand*, 2002] suggested the existence of a spatially broad, high-velocity anomaly in the top 100 km located beneath the SMC. *Abdelsalam et al.* [2011] interpreted those high-velocity anomalies from 0 to 100 km

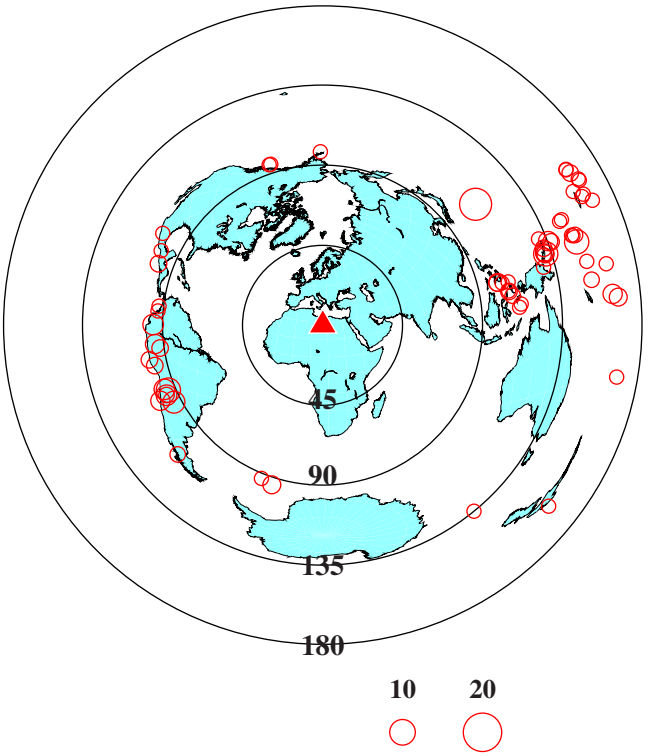

Figure 2. An azimuthal equidistant projection map of the Earth showing the distribution of earthquakes used in this study (red circles). The center of the study area is designated by a solid red triangle. The size of the circles corresponds directly to the number of high-quality SWS measurements obtained from each individual event.

depth as indicative of the reworked lithosphere of the SMC, while low velocities from depths of 100–175 km reflect the asthenosphere and are due to delamination of the cratonic root.

Only a sparse collection of SWS studies have been conducted in north central Africa [*Barruol and Hoffmann*, 1999; *Barruol and Ismail*, 2001; *Schmid et al*., 2004]. *Barruol and Hoffmann* [1999] measured XKS splitting parameters for station TAM on the Hoggar swell in Algeria (Figure 1), and they reported a station-averaged ϕ of $173\pm2^{\circ}$ and a δt of 0.88 ± 0.02 s. They also discovered a variation in fast direction with back azimuth, suggesting the presence of complex anisotropic layering beneath the Hoggar swell. Their model attributes the orientation of the upper layer of anisotropy to the N-S strike of regional shear zones related to Pan-African orogenesis, while the lower layer is fixed at 40° from the north, which is assumed to be induced by basal tectonic drag associated with the movement of the African plate toward the NE in a fixed hotspot reference frame. These observations were further confirmed with additional seismic data for station TAM by *Barruol and Ismail* [2001]. North African mantle anisotropy was studied by *Schmid et al*. [2004] by measuring SKS splitting parameters along the Mediterranean margins including two stations in northern Libya (Figure 1). They observed dominantly ENE-WSW fast orientations across the western Mediterranean, a nearly N-S fast orientation at the station in NW Libya, and a ENE orientation at the station in NE Libya (Figure 1). Anisotropic surface wave tomography results indicate dominantly N-S fast polarizations with slight NNE-SSW and NNW-SSE deviations for north central Africa [*Wüstefeld et al*., 2009]. These results are consistent with previous surface wave tomography-generated north-south fast orientations at depths of 200 km or greater attributed to asthenospheric flow [*Montagner et al*., 2007].

The Red Sea and adjacent terranes, namely the Arabian Shield and Dead Sea Transform, are shown to exhibit a first-order N-S polarization direction which is postulated to result from either coherent lithospheric strike-slip deformation [*Schmid et al*., 2004] or by northward movement of the lithosphere relative to the asthenosphere [*Elsheikh et al*., 2014]. Coincident with the study of *Schmid et al*. [2004], southern Iberia and Morocco are characterized by primarily E-W fast directions, while N-S measurements are only observed within the immediate vicinity of Gibralter [*Miller et al*., 2013]. *Miller et al*. [2013] interpret these findings as the combination of fossil anisotropy and modulation of mantle flow by the topography of the bottom of the lithosphere, as well as toroidal slab modulated flow.

2. Data and Methods

We utilize all three-component broadband data recorded by 15 stations available to us from the Libyan Center for Remote Sensing and Space Science recorded between early 2005 through 2007. We also include two permanent broadband seismic stations located in Libya, two in eastern Tunisia, and one in Algeria which acquired

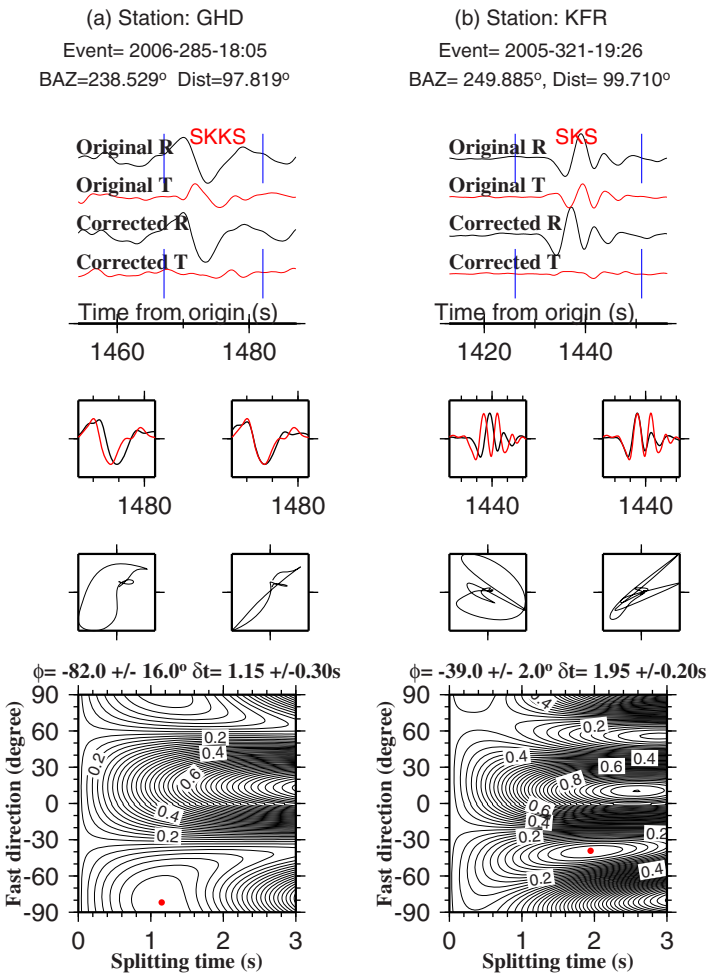

Figure 3. Examples of quality A measurements, showing the (top) original and corrected radial and transverse components, (middle) fast and slow components, and associated particle motion patterns prior to and following forwarding the slow component by the optimal splitting time, and (bottom) the corresponding error functions recorded by stations (left) GHD and (right) KFR.

data from early 1990 to 2014 and were archived at the IRIS (Incorporated Institutions for Seismology) DMC (Data Management Center). In this study, we use three core-mantle boundary P-to-S converted phases (PKS, SKKS, and SKS, collectively known as XKS) in order to maximize the coverage provided by the data. The useful epicentral ranges for the PKS, SKKS, and SKS phases are 120°–180°, 84°–180°, and 95°–180°, respectively [*Liu and Gao*, 2013]. Figure 2 shows the distribution of earthquakes used in this study and the quantity of high-quality measurements obtained from each event.

We apply the procedure developed by *Liu* [2009] and *Liu and Gao* [2013] based upon the minimization of transverse energy method [*Silver and Chan*, 1991] to calculate the splitting parameters. The requested seismograms are first band-pass filtered in the frequency range of 0.04–0.5 Hz to reject those with low signal-to-noise ratios (S/N). Detailed information about the definition of the parameters used to compute the S/N can be found in *Liu and Gao* [2013]. Each measurement is manually checked and assigned a rank of A (excellent), B (good), C (poor), or N (null). Rankings are assigned based on the S/N ratio of the original radial, original transverse, and corrected transverse components as well as the linearity of postminimization particle motion patterns and quality of the corrected transverse component (see *Liu et al.* [2008] for quantitative definitions of the rankings). Example measurements are shown in Figures 3 and 4. Finally, we explore the existence of complex anisotropy by examining the variation of the optimal pairs of splitting parameters with the back azimuth (BAZ).

3. Results

A total of 583 pairs of well-defined (quality A and B) parameters were obtained from 20 seismic stations throughout the study region, among which 369 are SKS, 144 are SKKS, and 70 are PKS measurements. The station-averaged splitting parameters, which are in general agreement with those obtained by previous studies at the three stations in the study area (Figure 1), are given in Table 1. At all but one (KFR, see below) of the stations, no discernible variation in the splitting parameters with BAZ is observed (Figure 5), suggesting that a single layer of anisotropy with a horizontal axis of symmetry underlies the study area, as is exemplified by the results at station JFR (Figure 6).

The fast orientations are dominantly N-S throughout most of the study area, though they change substantially to E-W at stations MRJ and MARJ in the northeastern coastal region and GHD in eastern Algeria (Figure

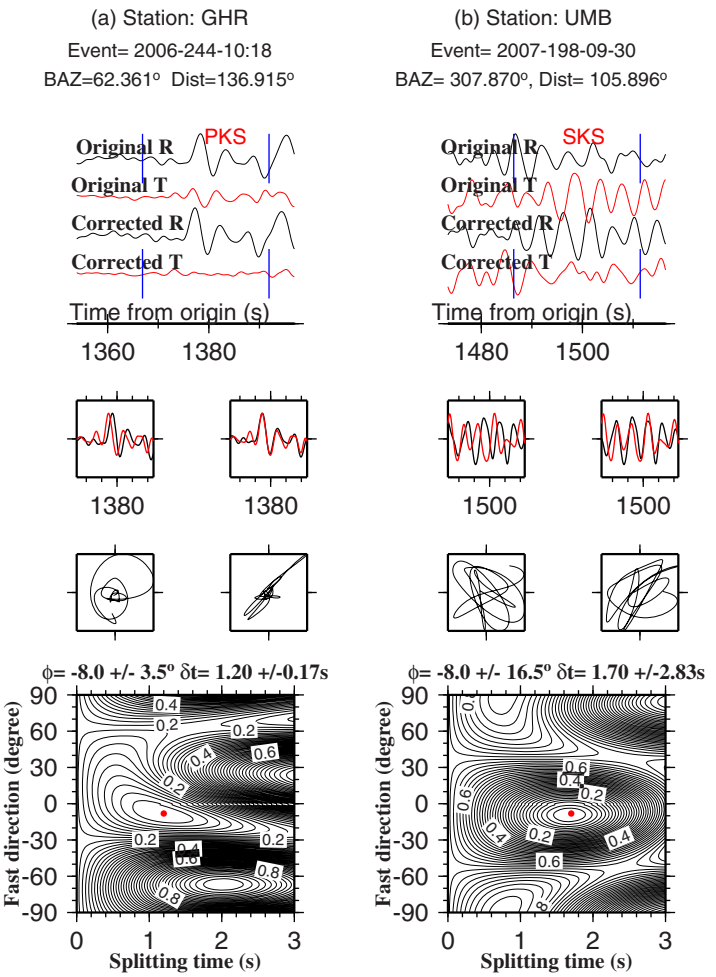

Figure 4. Same as Figure 3, but for a (left) rank B, and (right) rank C measurement recorded by stations GHR and UMB.

5). The station-averaged splitting times in the study area vary from 0.8 to 1.5 s (Table 1) with an overall mean splitting time of 1.2 ± 0.36 s, which is slightly higher than the global average delay time of 1.0 s [*Silver*, 1996]. Our delay average corresponds either to a 178 km thick layer with 3% anisotropy or a 133 km thick layer with 4% anisotropy. The largest station-averaged splitting times (greater than 1.3 s) are observed primarily in the northwestern and central areas of the study region. Splitting measurements recorded by stations within the volcanic areas (Figure 1) do not display any significant anomalies in the orientation and splitting time values.

4. Discussion

4.1. Estimation of the Depth of Anisotropy

One of the drawbacks of using SWS measurements to constrain anisotropic structure is the lack of vertical resolution, especially when the distance between the stations is large (e.g., more than about 70 km) and thus the technique of

Table 1. Station-Averaged Splitting Parameters

Station Name	Lon. (°)	Lat. (°)	ϕ (°)	δt (s)	No. of Events
ASA	11.370	32.510	151 ± 18	1.10 ± 0.26	28
GFA	9.070	34.340	6 ± 21	1.45 ± 0.32	5
GHAR	13.090	32.120	154 ± 11	1.36 ± 0.41	59
GHD	9.270	30.010	89 ± 14	0.90 ± 0.23	20
GHR	13.050	32.070	151 ± 13	1.26 ± 0.35	41
JDB	20.120	30.550	26 ± 8	0.91 ± 0.21	18
JFR	15.490	29.060	16 ± 7	1.52 ± 0.25	40
KFR	23.130	24.100	32 ± 45	1.14 ± 0.42	31
MARJ	20.880	32.520	66 ± 12	0.80 ± 0.23	1
MRJ	20.530	32.350	74 ± 13	1.12 ± 0.32	7
MSR	15.010	32.190	18 ± 18	1.01 ± 0.25	37
SHF	14.150	29.590	142 ± 7	1.33 ± 0.21	15
SRT	16.390	31.050	38 ± 14	1.43 ± 0.37	28
TAM	5.530	22.790	176 ± 7	1.00 ± 0.35	129
TATN	10.530	32.580	175 ± 11	1.38 ± 0.40	36
TBQ	23.550	32.030	172 ± 12	1.21 ± 0.38	6
TRP	13.100	32.510	1 ± 12	0.81 ± 0.20	6
UJL	21.180	29.070	155 ± 11	1.33 ± 0.47	24
UMB	14.450	26.080	24 ± 12	1.17 ± 0.26	34
ZLA	17.340	28.330	18 ± 9	0.82 ± 0.30	18

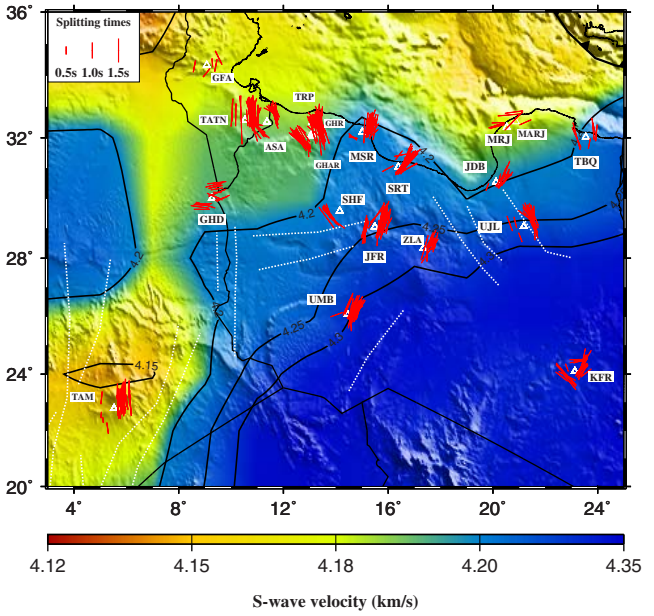

Figure 5. Map illustrating global *S* wave tomography results for our study area for the depth range of 0–100 km from the *Grand* [2002] model. Red bars are high-quality (rankings A and B) SWS parameters from this study (plotted above the 200 km piercing points). Contour lines are spaced at 0.05 km/s intervals.

spatial coherency of splitting parameters [*Liu and Gao*, 2011] cannot be applied. One of the stations, KFR in the SE corner of the study area (Figure 5), shows strong azimuthal dependence (Figure 7) that is not characterized by either a 90° or 180° periodicity (the former is diagnostic of multiple-layer anisotropy, while the latter may indicate a single layer with a dipping axis). Instead, XKS arrivals from the NE quadrant show a mostly NE fast orientation, while those from the west show a NW fast orientation (Figure 7), suggesting that the first Fresnel zones from the two groups of events do not significantly overlap with each other [*Alsina and Snieder*, 1995]. By using a typical XKS ray parameter of 5.4 s/degree and a dominant period of 6.67 s, we estimate that the center of the source of anisotropy beneath the station must be deeper than 200 km. At this depth, the first Fresnel zone has a diameter of about 110 km, and the ray-piercing points between the two groups of events is about 90 km apart, i.e., there is a slight partial overlap at this depth. A complete separation of the two Fresnel zones occurs at the depth of about 275 km. Interestingly, for some of the events recorded by this station, the optimal splitting parameters cannot completely remove the energy on the corrected transverse component (see Figure 3b, for example). One possible explanation is that the Fresnel zones for the XKS waves from these events partially overlap, and thus, the waveforms are influenced by both regions of anisotropy.

4.2. Relationship With Lithospheric Fabrics

Coherent lithospheric deformation during active collisional tectonism may lead to the development of anisotropic alignment "frozen" into the lithosphere, otherwise known as fossil anisotropy [*Bormann et al*., 1993; *Silver*, 1996]. Consequently, orogenic belts are often characterized by fast orientations which parallel the strike of the mountain range [*McNamara et al*., 1994], which in turn reflects the mineralogical fabrics orthogonal to the direction of shortening [*Vinnik et al*., 1992; *Silver*, 1996; *Gao et al*., 1997; *Savage*, 1999; *Walker et al*., 2004].

The dominantly N-S fast orientations observed within our study area do not support the fossil anisotropy model, primarily because the observed fast orientations at most of the stations do not parallel the strike of regional structural features (Figure 1). This lack of correlation is especially emphasized by the dominantly E-W polarization observed beneath station GHD, which is in the N-S striking TSO, and by the near-orthogonal relationship between the N-S fast orientation detected at stations JFR and SHF and the nearby ENE-WSW trending structural trends (Figure 5). Additionally, splitting delay times do not show a clear dependency upon variations in seismic tomographic anomalies as reported by *Grand* [2002] (Figure 5), whereas inherent lateral velocity heterogeneities in the lithosphere are expected to induce a diverse range of possible splitting times dependent upon local tectonic influence. Under the hypothesis of lithospheric anisotropy, in regions with thicker lithosphere, the splitting times should be higher. This correspondence is not observed (Figure 5). A lithospheric origin is also inconsistent with a sublithospheric depth of the source of anisotropy estimated using the Fresnel zone approach in the preceding section, using data from a single station. However, due to a lack of high-resolution characterization of lithospheric structure beneath the study area, significant lithospheric contributions cannot be completely ruled out at the present time.

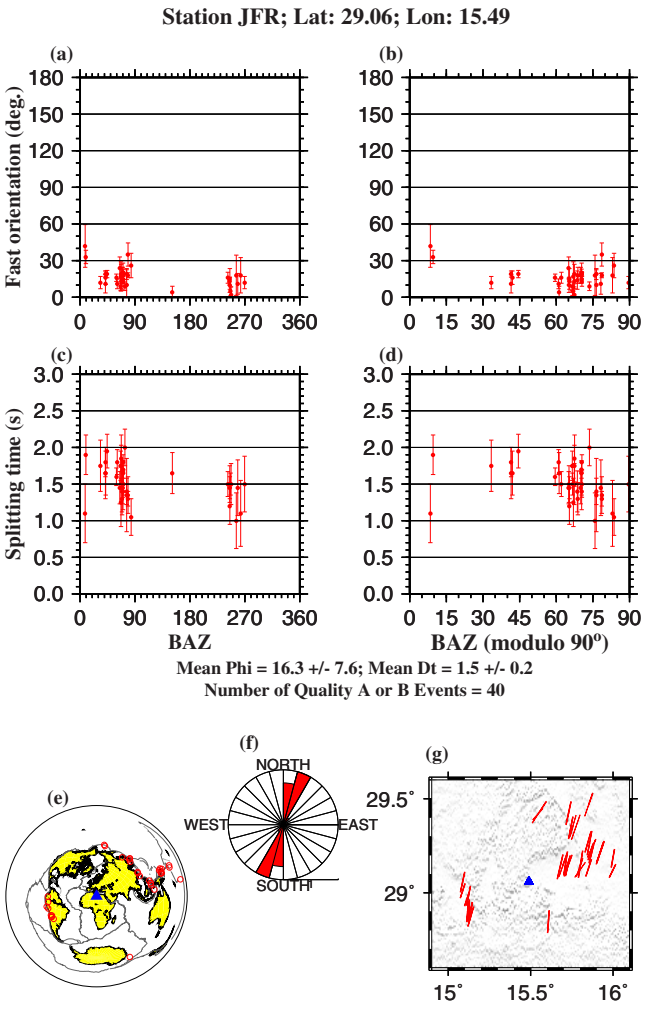

Figure 6. Summary of measurements at station JFR. (a) Azimuthal variations of the fast orientation ϕ plotted against back azimuth; (b) fast orientation plotted against modulo-90° back azimuth; (c and d) same as Figures 6a and 6b but for splitting times; (e) an azimuthal equidistant projection map illustrating distribution of XKS events used for the station; (f) a normalized rose diagram illustrating distribution of fast orientations; (g) splitting parameters plotted above ray-piercing points at 200 km depth. The triangle represents the station.

4.3. APM-Related Anisotropy

When the lithosphere moves on top of a stationary asthenosphere, or when both layers move in the APM direction with different speeds, simple shear in the boundary layer between the lithosphere and asthenosphere can lead to APM-parallel fast orientations [*Zhang and Karato*, 1995; *Tommasi et al*., 1996; *Tommasi*, 1998; *Walker et al*., 2004; *Barruol and Fontaine*, 2013; *Liu et al*., 2014]. The fixed hot spot model (HS3-NUVEL1A) of *Gripp and Gordon* [2002] suggests a velocity of 2 cm/yr approximately toward the west for north central Africa (Figure 1). With few exceptions, the observed splitting measurements show N-S predominance and are largely orthogonal to the APM, implying that neither of the assumptions (stationary asthenosphere or APM-parallel differential motions of both layers) applies to the study area.

4.4. Anisotropy Induced by Long-Term Relative Plate Motion

Several studies have proposed that the African plate has been moving northward relative to Eurasia since at least 150 Ma, primarily as the result of northward subduction of Neotethys oceanic lithosphere beneath Eurasia [*Dercourt et al*., 1986; *Reilinger and McClusky*, 2011]. N-S oriented simple shear consequently formed in the boundary layer between the lithosphere and the asthenosphere is used by *Elsheikh et al*. [2014] to explain the dominantly N-S fast orientations observed in the vicinity of the northern Red Sea (Figure 1). This model, when combined with the influence of the topography of the bottom of the lithosphere (Figure 5), can explain the observed splitting parameters in our study area. The spatial distribution of *S* wave velocities in the top 100 km (Figure 5) [*Grand*, 2002] suggests a northward thinning of the lithosphere, although the exact 3-D geometry of the edge of the continental root cannot be imaged due to a lack of high-resolution geophysical data. Interestingly, the three stations showing a dominantly E-W fast orientation are all located near the northern end of the E-W zone of a strong velocity gradient (Figure 5). Under the assumption that this zone represents the approximate edge of the African continental root, E-W oriented asthenospheric flow locally deflected by the root can explain the E-W fast orientations. Such a modulation of mantle flow by a continental root has been used to explain edge-parallel fast orientations around the western and southern edges of the North American continental root [*Fouch et al*., 2000; *Refayee et al*., 2014; *Yang et al*., 2014]. It has also been suggested beneath central America [*Miller and Becker*, 2012] and NW Africa [*Miller et al*., 2013]. It must be emphasized that due to a near paucity of available broadband seismic data (until recently) in the interior of north central Africa, high-resolution images of upper-mantle structure, which are critical constraints for reliable interpretations of SWS observations, are still absent. In general, our observations suggest that relative to the asthenosphere, the

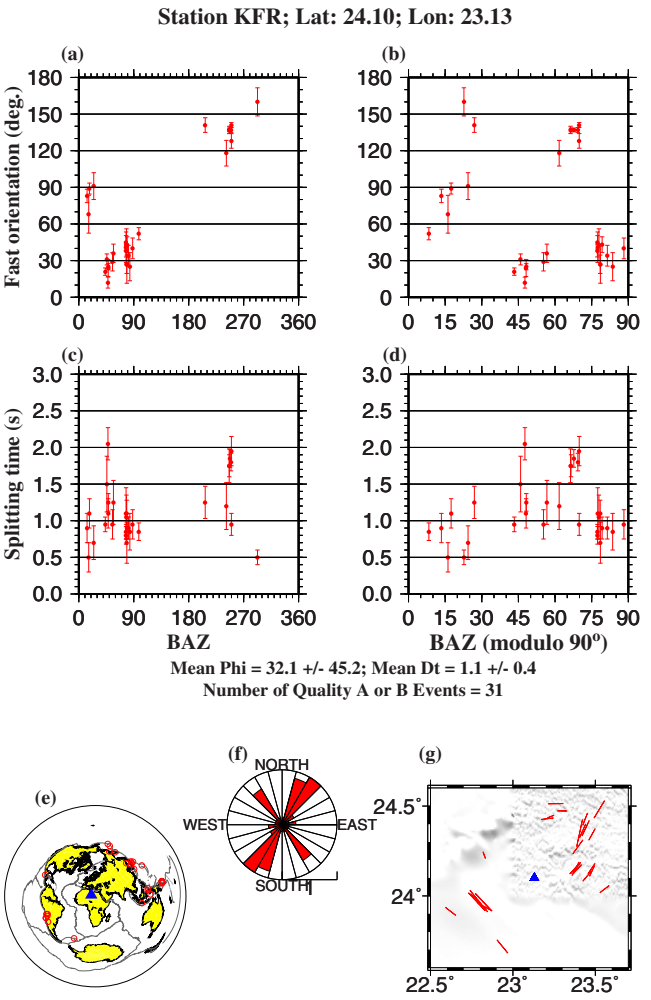

Figure 7. Same as Figure 6, but for station KFR.

lithosphere in north central Africa is moving toward the north or south, giving rise to primarily N-S fast orientations.

5. Conclusions

For the first time, shear wave splitting parameters are measured at seismic stations in the interior of Libya, from which data have been previously unavailable. Observed fast polarization orientations in north central Africa are dominantly N-S at most of the stations, and E-W at the rest. The source of anisotropy is estimated to be in the upper asthenosphere based on the nonperiodic azimuthal variation of splitting parameters observed at one of the stations. This observation, when combined with the significant discrepancies between the resulting fast orientations and dominant trends of tectonic features, suggests a primarily asthenospheric origin of the observed anisotropy. Our preferred model includes a differential velocity between the lithosphere and the asthenosphere along the N-S direction that leads to simple shear in the lithosphere-asthenosphere boundary layer, as well as deflection of mantle flow by the E-W trending northern edge of the root of the African continent.

Acknowledgments

Data used for the study were obtained from two sources: (1). Libyan Center for Remote Sensing and Space Science (LCRSSS) and (2) the IRIS DMC. The original and corrected XKS waveforms and other related data used to produce results at the LCRSSS stations can be freely accessed at http://r08sgao.managed.mst.edu/libyasws/all/meas.html, and data from the IRIS DMC are publicly accessible. The study was supported by the Benghazi University of Libya and Statoil of Norway through research grants to K.L. and S.G.

References

Abdelsalam, M. G., S. S. Gao, and J.-P. Liégeois (2011), Upper mantle structure of the Saharan Metacraton, *J. Afr. Earth Sci.*, *60*, 328–336, doi:10.1016/j.jafrearsci.2011.03.009.

Alsina, D., and R. Snieder (1995), Small-scale sublithospheric continental mantle deformation: Constraints from *SKS* splitting observations, *Geophys. J. Int.*, *123*, 431–448.

Barruol, G., and F. R. Fontaine (2013), Mantle flow beneath La Réunion hotspot track from SKS splitting, *Earth Planet. Sci. Lett.*, *362*, 108–121, doi:10.1016/j.epsl.2012.11.017.

Barruol, G., and R. Hoffmann (1999), Upper mantle anisotropy beneath the Geoscope stations, *J. Geophys. Res.*, *104*, 10,757–10,773, doi:10.1029/1999JB900033.

Barruol, G., and W. B. Ismail (2001), Upper mantle anisotropy beneath the African IRIS and Geoscope stations, *J. Geophys. Int.*, *146*(2), 549–561, doi:10.1046/j.0956-540x.2001.01481.x.

Becker, T. W., and R. J. O'Connell (2001), Predicting plate velocities with mantle circulation models, *Geochem. Geophys. Geosyst. 2(12)*, *1060*, doi:10.1029/2001GC000171.

Becker, T. W., V. Schulte-Pelkum, D. K. Blackman, J. B. Kellogg, and R. J. O'Connell (2006), Mantle flow under the western United States from shear wave splitting, *Earth Planet. Sci. Lett.*, *247*, 235–251, doi:10.1016/j.epsl.2006.05.010.

Bird, P., Z. Liu, and W. K. Rucker (2008), Stresses that drive the plates from below: Definitions, computational path, model optimization, and error analysis, *J. Geophys. Res.*, *113*, B11406, doi:10.1029/2007JB005460.

Bormann, P., P. T. Burghardt, L. I. Makeyeva, and L. P. Vinnik (1993), Teleseismic shear-wave splitting and deformations in Central Europe, *Phys. Earth Planet. Inter.*, *78*(3), 157–166, doi:10.1016/0031-9201(93)90153-Z.

Buontempo, L., G. H. R. Bokelmann, G. Barruol, and J. Morales (2008), Seismic anisotropy beneath southern Iberia from SKS splitting, *Earth Planet. Sci. Lett.*, *273*(3), 237–250, doi:10.1016/j.epsl.2008.06.024.

Conrad, C. P., and M. D. Behn (2010), Constraints on lithosphere net rotation and asthenospheric viscosity from global mantle flow models and seismic anisotropy, *Geochem. Geophys. Geosyst.*, *11*, Q05W05, doi:10.1029/2009GC002970.

DeMets, C., R. G. Gordon, D. F. Argus, and S. Stein (1994), Effect of recent revisions to the geomagnetic reversal time scale on estimates of current plate motions, *Geophys. Res. Lett.*, *21*, 2191–2194, doi:10.1029/94GL02118.

Dercourt, J., et al. (1986), Geological evolution of the Tethys belt from the Atlantic to the Pamirs since the LIAS, *Tectonophysics*, *123*, 241–315, doi:10.1016/0040-1951(86)90199-X.

Diaz, J., and J. Gallart (2014), Seismic anisotropy from the Variscan core of Iberia to the Western African Craton: New constrains on upper mantle flow at regional scales, *Earth Planet. Sci. Lett.*, *394*, 48–57, doi:10.1016/j.epsl.2014.03.005.

Diaz, J., J. Gallart, A. Hirn, and H. Paulssen (1998), Anisotropy beneath the Iberian Peninsula: The contribution of the ILIHA-NARS broad-band experiment, *Pure Appl. Geophys.*, *151*, 395–405.

Diaz, J., J. Gallart, A. Villaseor, F. Mancilla, A. Pazos, D. Crdoba, J. A. Pulgar, P. Ibarra, and M. Harnafi (2010), Mantle dynamics beneath the Gibraltar Arc (western Mediterranean) from shear-wave splitting measurements on a dense seismic array, *Geophys. Res. Lett.*, *37*, L18304, doi:10.1029/2010GL044201.

Doglioni, C., A. Ismail-Zadeh, G. Panza, and F. Riguzzi (2011), Lithosphere-asthenosphere viscosity contrast and decoupling, *Phys. Earth Planet. Inter.*, *189*, 1–8, doi:10.1016/j.pepi.2011.09.006.

Elsheikh, A. A., S. S. Gao, K. H. Liu, A. A. Mohamed, Y. Yu, and R. E. Fat-Helbary (2014), Seismic anisotropy and subduction-induced mantle fabrics beneath the Arabian and Nubian Plates adjacent to the Red Sea, *Geophys. Res. Lett.*, *41*, 2376–2381, doi:10.1002/2014GL059536.

Faccenna, C., and T. W. Becker (2010), Shaping mobile belts by small-scale convection, *Nature*, *465*, 602–605, doi:10.1038/nature09064.

Faccenna, C., et al. (2014), Mantle dynamics in the Mediterranean, *Rev. Geophys.*, *52*, 283–332, doi:10.1002/2013RG000444.

Forte, A. M., S. Quéré, R. Moucha, N. A. Simmons, S. P. Grand, J. X. Mitrovica, and D. B. Rowley (2010), Joint seismic-geodynamic-mineral physical modelling of African geodynamics: A reconciliation of deep-mantle convection with surface geophysical constraints, *Earth Planet. Sci. Lett.*, *295*, 329–341, doi:10.1016/j.epsl.2010.03.017.

Fouch, M. J., K. M. Fischer, E. M. Parmentier, M. E. Wysession, and T. J. Clarke (2000), Shear wave splitting, continental keels, and patterns of mantle flow, *Geophys. J. Res.*, *105*, 6255–6275, doi:10.1029/1999JB900372.

Gao, S., P. M. Davis, H. Liu, P. D. Slack, A. W. Rigor, Y. A. Zorin, V. V. Mordvinova, V. M. Kozhevnikov, and N. A. Logatchev (1997), SKS splitting beneath continental rift zones, *J. Geophys. Res.*, *102*, 22,781–22,797, doi:10.1029/97JB01858.

Grand, S. P. (2002), Mantle shear-wave tomography and the fate of subducted slabs, *Philos. Trans. R. Soc. London A*, *360*, 2475–2491, doi:10.1098/rsta.2002.1077.

Gripp, A. E., and R. G. Gordon (2002), Young tracks of hotspots and current plate velocities, *Geophys. J. Int.*, *150*, 321–361, doi:10.1046/j.1365-246X.2002.01627.x.

Guiraud, R., and W. Bosworth (1997), Senonian basin inversion and rejuvenation of rifting in Africa and Arabia: Synthesis and implications to plate-scale tectonics, *Tectonophysics*, *282*, 39–82, doi:10.1016/S0040–1951(97)00212-6.

Hassan, H. S., and C. G. Kendall (2014), Hydrocarbon provinces in Libya: A petroleum system study, in *Petroleum Systems of the Tethyan Region, AAPG Mem.*, vol. 106, edited by L. Marlow, C. Kendall, and L. Yose, pp. 101–142, Tulsa, Oklahoma, USA.

Hansen, S. E., S. Schwartz, A. Al-Amri, and A. Rodgers (2006), Combined plate motion and density-driven flow in the asthenosphere beneath Saudi Arabia: Evidence from shear-wave splitting and seismic anisotropy, *Geology*., 34, 869–872, doi:10.1130/G22713.1.

Karato, S., H. Jung, I. Katayama, and P. Skemer (2008), Geodynamic significance of the seismic anisotropy of the upper mantle: New insights from laboratory studies, *Annu. Rev. Earth Planet. Sci.*, *36*, 59–95, doi:10.1146/annurev.earth.36.031207.124120.

Kaviani, A., G. Rumpker, M. Weber, and G. Asch (2011), Short-scale variations of shear-wave splitting across the Dead Sea basin: Evidence for the effects of sedimentary fill, *Geophys. Res. Lett.*, *38*, L04308, doi:10.1029/2010GL046464.

Kaviani, A., R. Hofstetter, G. Rümpker, and M. Weber (2013), Investigation of seismic anisotropy beneath the Dead Sea fault using dense networks of broadband stations, *J. Geophys. Res. Solid Earth*, *118*, 3476–3491, doi:10.1002/jgrb.50250.

Kreemer, C. (2009), Absolute plate motions constrained by shear wave splitting orientations with implications for hot spot motions and mantle flow, *J. Geophys. Res.*, *114*, B10405, doi:10.1029/2009JB006416.

Liégeois, J. P., L. Latouche, M. Boughrara, J. Navez, and M. Guiraud (2003), The LATEA (Central Hoggar, Tuareg shield, Algeria): Behavior of an old passive margin during the Pan-African orogeny, *J. Afr. Earth Sci.*, *37*, 161–190, doi:10.1016/j.jafrearsci.2003.05.004.

Liu, K. H. (2009), NA-SWS-1.1: A uniform database of teleseismic shear wave splitting measurements for North America, *Geochem. Geophys. Geosyst.*, *10*, Q05011, doi:10.1029/2009GC002440.

Liu, K. H., and S. S. Gao (2011), Estimation of the depth of anisotropy using spatial coherency of shear-wave splitting parameters, *Bull. Seismol. Soc. Am.*, *101*, 2153–2161, doi:10.1785/0120100258.

Liu, K. H., and S. S. Gao (2013), Making reliable shear-wave splitting measurements, *Bull. Seismol. Soc. Am.*, *103*(5), 2680–2693, doi:10.1785/0120120355.

Liu, K. H., S. S. Gao, Y. Gao, and J. Wu (2008), Shear-wave splitting and mantle flow associated with the deflected Pacific slab beneath northeast Asia, *J. Geophys. Res.*, *113*, B01305, doi:10.1029/2007JB005178.

Liu, K. H., A. Elsheikh, A. Lemnifi, U. Purevsuren, M. Ray, H. Refayee, B. Yang, Y. Yu and S. S. Gao (2014), A uniform database of teleseismic shear wave splitting measurements for the western and central United States, *Geochem. Geophys. Geosyst.*, *15*, 2075–2085, doi:10.1002/2014GC005267.

Marone, F., and B. Romanowicz (2007), The depth distribution of azimuthal anisotropy in the continental upper mantle, *Nature*, *447*, 198–201, doi:10.1038/nature05742.

McNamara, D. E., T. J. Owens, P. G. Silver, and F. T. Wu (1994), Shear wave anisotropy beneath the Tibetan Plateau, *J. Geophys. Res.*, *99*, 13,655–13,665, doi:10.1029/93JB03406.

Meert, J. G., and B. S. Lieberman (2008), The Neoproterozoic assembly of Gondwana and its relationship to the Ediacaran-Cambrian radiation, *Gondwana Res.*, *14*, 5–21, doi:10.1016/j.gr.2007.06.007.

Miller, M. S., and T. W. Becker (2012), Mantle flow deflected by interactions between subducted slabs and cratonic keels, *Nature*, *5*, 726–730, doi:10.1038/ngeo1553.

Miller, M. S., A. A. Allam, T. W. Becker, J. F. Di Leo, and J. Wookey (2013), Constraints on the tectonic evolution of the westernmost Mediterranean and northwestern Africa from shear wave splitting analysis, *Earth Planet. Sci. Lett.*, *375*, 234–243, doi:10.1016/j.epsl.2013.05.036.

Montagner, J.-P., B. Marty, E. Stutzmann, D. Sicilia, M. Cara, R. Pik, J.-J. Lévêque, G. Roult, E. Beucler, and E. Debayle (2007), Mantle upwellings and convective instabilities revealed by seismic tomography and helium isotope geochemistry beneath eastern Africa, *Geophys. Res. Lett.*, *34*, L21303, doi:10.10129/2007GL031098.

Refayee, H. A., B. B. Yang, K. H. Liu, and S. S. Gao (2014), Mantle flow and lithosphere-asthenosphere coupling beneath the southwestern edge of the North American craton: Constrains from shear-wave splitting measurements, *Earth Planet. Sci. Lett.*, *402*, 209–220, doi:10.1016/j.epsl.2013.01.031i.

Reilinger, R., and S. McClusky (2011), Nubia-Arabia-Eurasia plate motions and the dynamics of Mediterranean and Middle East tectonics, *Geophys. J. Int.*, *186*, 971–979, doi:10.1111/j.1365-246X.2011.05133.x.

Salah, M. K. (2012), A seismological evidence for the northwestward movement of Africa with respect to Iberia from shear-wave splitting, *Geosci. Frontiers*, *3*(5), 681–696, doi:10.1016/j.gsf.2012.01.005.

Savage, M. K. (1999), Seismic anisotropy and mantle deformation: What have we learned from shear wave splitting?, *Rev. Geophys.*, *37*, 65–106, doi:10.1029/98RG02075.

Schaefer, J. F., L. Boschi, T. W. Becker, and E. Kissling (2011), Radial anisotropy in the European mantle: Tomographic studies explored in terms of mantle flow, *Geophys. Res. Lett.*, *38*, L23304, doi:10.1029/2011GL049687.

Schmid, C., S. Van Der Lee, and D. Giardini (2004), Delay times and shear wave splitting in the Mediterranean region, *Geophys. J. Int.*, *159*, 275–290, doi:10.1111/j.1365-246X.2004.02381.x.

Silver, P. G. (1996), Seismic anisotropy beneath the continents: Probing the depths of geology, *Annu. Rev. Earth Planet. Sci.*, *24*, 385–432.

Silver, P. G., and W. W. Chan (1991), Shear wave splitting and subcontinental mantle deformation, *J. Geophys. Res.*, *96*, 16,429–16,454, doi:10.1029/91JB00899.

Stern, R. J. (1994), Arc assembly and continental collision in the Neoproterozoic East African Orogen: Implications for the consolidation of Gondwanaland, *Annu. Rev. Earth Planet. Sci.*, *22*, 319–351.

Stoeser, D. B., and V. E. Camp (1985), Pan-African microplate accretion of the Arabian Shield, *Geol. Soc. Am. Bull.*, *96*, 817–826, doi:10.1130/0016–7606(1985)96<817:PMAOTA>2.0.CO;2.

Tommasi, A. (1998), Forward modeling of the development of seismic anisotropy in the upper mantle, *Earth Planet. Sci. Lett.*, *160*(1), 1–13, doi:10.1016/S0012–821X(98)00081-8.

Tommasi, A., A. Vauchez, and R. Russo (1996), Seismic anisotropy in ocean basins: Resistive drag of the sublithospheric mantle?, *Geophys. Res. Lett.*, *23*, 2991–2994, doi:10.1029/96GL02891.

Vinnik, L. P., L. I. Makeyeva, A. Milev, and A. Y. Usenko (1992), Global patterns of azimuthal anisotropy and deformations in the continental mantle, *Geophys. J. Int.*, *111*, 433–447, doi:10.1111/j.1365-246X.1992.tb02102.

Walker, K. T., A. A. Nyblade, S. L. Klemperer, G. H. Bokelmann, and T. J. Owens (2004), On the relationship between extension and anisotropy: Constraints from shear wave splitting across the East African Plateau, *Geophys. J. Res.*, *109*, B08302, doi:10.1029/2003JB002866.

Wüstefeld, A., G. H. R. Bokelmann, G. Barruol, and J. P. Montagner (2009), Identifying global seismic anisotropy patterns by correlating shear-wave splitting and surface-wave data, *Phys. Earth Planet. Inter.*, *176*, 198–212, doi:10.1016/j.pepi.2009.05.006.

Yang, B. B., S. S. Gao, K. H. Liu, A. A. Elsheikh, A. A. Lemnifi, H. A. Refayee, and Y. Yu (2014), Seismic anisotropy and mantle flow beneath the northern Great Plains of North America, *J. Geophys. Res.*, *119*, 2138–2152, doi:10.1002/2013JB010719.

Zhang, S., and S. I. Karato (1995), Lattice preferred orientation of olivine aggregates deformed in simple shear, *Nature*, *375*(6534), 774–777, doi:10.1038/375774a0.